

# Study of sensitization process on mid-infrared uncooled PbSe photoconductive detectors leads to high detectivity

Cite as: J. Appl. Phys. **113**, 103102 (2013); <https://doi.org/10.1063/1.4794492>

Submitted: 18 December 2012 . Accepted: 21 February 2013 . Published Online: 11 March 2013

Jijun Qiu, Binbin Weng, Zijian Yuan, and Zhisheng Shi



View Online



Export Citation



CrossMark

## ARTICLES YOU MAY BE INTERESTED IN

[Understanding sensitization behavior of lead selenide photoconductive detectors by charge separation model](#)

Journal of Applied Physics **115**, 084502 (2014); <https://doi.org/10.1063/1.4867038>

[CdS/PbSe heterojunction for high temperature mid-infrared photovoltaic detector applications](#)

Applied Physics Letters **104**, 121111 (2014); <https://doi.org/10.1063/1.4869752>

[Responsivity enhancement of mid-infrared PbSe detectors using CaF<sub>2</sub> nano-structured antireflective coatings](#)

Applied Physics Letters **104**, 021109 (2014); <https://doi.org/10.1063/1.4861186>

Lock-in Amplifiers  
up to 600 MHz



Watch



## Study of sensitization process on mid-infrared uncooled PbSe photoconductive detectors leads to high detectivity

Jijun Qiu,<sup>1,a)</sup> Binbin Weng,<sup>1,a)</sup> Zijian Yuan,<sup>1</sup> and Zhisheng Shi<sup>1,2,b)</sup>

<sup>1</sup>*School of Electrical and Computer Engineering, University of Oklahoma, Norman, Oklahoma 73019, USA*

<sup>2</sup>*Nanolight, Inc., Norman, Oklahoma 73069, USA*

(Received 18 December 2012; accepted 21 February 2013; published online 11 March 2013)

For nearly a century, oxygen has been widely accepted as the key element that triggers photo-response in polycrystalline PbSe photoconductive detectors. Our photoluminescence and responsivity studies on PbSe samples, however, suggest that oxygen only serves as an effective sensitization improver and it is iodine rather than oxygen that plays the key role in triggering the photo-response. These studies shed light on the sensitization process for detector applications and ways to passivate defects in IV–VI semiconductors. As a result, high peak detectivity of  $2.8 \times 10^{10} \text{ cm} \cdot \text{Hz}^{1/2} \cdot \text{W}^{-1}$  was achieved at room temperature. © 2013 American Institute of Physics. [<http://dx.doi.org/10.1063/1.4794492>]

### I. INTRODUCTION

After many years' development since 1930s, uncooled PbS and PbSe polycrystalline photoconductive detectors remain the choice for many applications in the 1–5  $\mu\text{m}$  spectral range mainly due to their lower cost but comparable performance to their counterparts such as Hg<sub>1-x</sub>CdTe (MCT) detectors.<sup>1</sup> Regardless of deposition techniques, as-grown Pb-salt poly-crystalline films must be thermally treated at certain atmosphere to become sensitive to infrared radiation, being known as sensitization procedure. There is a broad scientific consensus that oxygen plays the key role in the sensitization process by introducing deep trap and/or forming p-n junction in PbSe crystallites. Great efforts have been made to explain the physical essence of sensitization both from theoretical studies and experimental phenomenology.<sup>2–7</sup>

Although the physical model of how these heuristic procedures lead to photoconductivity has not been unambiguously explained, the experimental fact after these sensitization processes is that carrier lifetime becomes extremely long (longer than  $\mu\text{s}$ ), and thus leads to a greatly enhanced photo-response. The carrier lifetime is much longer than any reported experimental and theoretical Auger and radiative lifetime.<sup>8</sup> For example, room temperature Auger and radiative lifetimes are in the range of tens to 100 ns calculated by Zogg for direct recombination in PbSe with  $n = 2.3 \times 10^{17} \text{ cm}^{-3}$  according to Emtage and Ziep.<sup>9–11</sup> Therefore, there must be a mechanism that has significantly inhibited the fast Auger and radiative recombination.

There are mainly two types of models which are related to a “generalized theory” discussed by Petriz.<sup>7</sup> The first model is that oxygen introduces minority carrier trap that effectively traps the photon-induced minority carriers. As is shown in equation below, when carrier concentration is significantly reduced Auger, radiative, and Shockley-Read-Hall (SRH) recombination will be significantly inhibited, leading to much enhanced lifetime and thus photo-response

$$R_{total} = r_{rad}np + r_{Aug-e}n^2p + r_{Aug-h}np^2 + \frac{n}{\tau_{SRH-e}} + \frac{p}{\tau_{SRH-h}}, \quad (1)$$

where  $R_{total}$  is total recombination rate,  $r_{rad}$  is radiative recombination coefficient,  $n$  is electrons concentration,  $p$  is holes concentration,  $r_{Aug-e}$  is Auger electrons recombination coefficient,  $r_{Aug-h}$  is Auger holes recombination coefficient,  $\tau_{SRH-e}$  is electrons lifetime of Shockley-Read-Hall recombination, and  $\tau_{SRH-h}$  is holes lifetime of Shockley-Read-Hall recombination.

The second model suggests formation of p-n junction during sensitization process.<sup>12</sup> Most of the reports suggested that sensitizer such as oxygen converts the n-type material into p-type material. The p-type inversion region at the outer layer of the microcrystal and the n-type material in the core forms a p-n junction. The built-in potential of the p-n junction spatially separates photon-induced electrons and holes in a rate faster than Auger and radiative recombination, and enhances the carrier lifetime. Trofimov suggested deep donor and acceptor states on grain surfaces.<sup>13</sup> The density of such states rises during oxidation of the semiconductor. The capture of majority carriers at such states gives rise to surface band bending, leading to the formation of a depletion layer near the surface of each crystallite, independent of the conductivity type. Similar concept was also introduced into MCT detectors in the 1980s, often referring as “trapping-mode photoconductors.”<sup>1</sup> For Pb-salt polycrystalline PC detectors, however, such suggested p-n junctions are on the interfaces of sub-micron scale crystallites, making direct confirmation of such model challenging.

Both models mentioned above would suggest that the radiative recombination after sensitization should be hindered, thus photoluminescence (PL) signal should be significantly suppressed. Our previous PL measurements on a series of PbSe thin films grown on a (111)-oriented Si substrate by molecular beam epitaxy (MBE) annealed with high-purity oxygen,<sup>14</sup> however, suggest otherwise. The PL intensity is increased significantly, rather than suppressed, after O<sub>2</sub> annealing.

<sup>a)</sup>Jijun Qiu and Binbin Weng contributed equally to this work.

<sup>b)</sup>Author to whom correspondence should be addressed. Electronic mail: shi@ou.edu.

In addition to oxygen, the role of halogen such as iodine, another critical element in PbSe sensitization process, remains unclear in the academic community. Humphrey pointed out that halogens can be used to convert a PbSe film from n-type to p-type,<sup>15,16</sup> with no effect in the sensitivity of PbSe films. The high sensitivity of PbSe was achieved only through the incorporation of oxygen. Torquemada indicated in their work of thermally deposited PbSe that halogen only behaves as a transport agent during the PbSe recrystallization process to promote the *in situ* incorporation of oxygen into the PbSe lattice in electrically active position.<sup>17</sup>

In this paper, we conduct responsivity and PL measurements on polycrystalline samples grown by chemical bath deposition (CBD) and sensitized under different atmospheres. Our results show that it is iodine instead of oxygen that plays the most critical role in the sensitization procedure of p-type PbSe photo-conductor. Oxygen, while still important, only serves as a very effective sensitization improver.

## II. EXPERIMENT

PbSe were fabricated on glass and (111) Si substrates by using CBD method. In brief, the aqueous precursor was prepared via dissolving sodium hydroxide, lead acetate, and selenosulfate with a concentration ratio of 12:1:1. The cleaned glass substrates were transferred into the aqueous precursor and maintained at 70 °C for 1.5 h. The as-grown PbSe films (sample I) show a compact structure with a large surface roughness, which is due to large particle sizes (about 0.7–1.2 μm) and various growth directions, as shown in Figure 1(a). To understand the essence of sensitization process, as-grown PbSe films were annealed in well-designed atmospheres at 380 °C for a constant total annealing time,

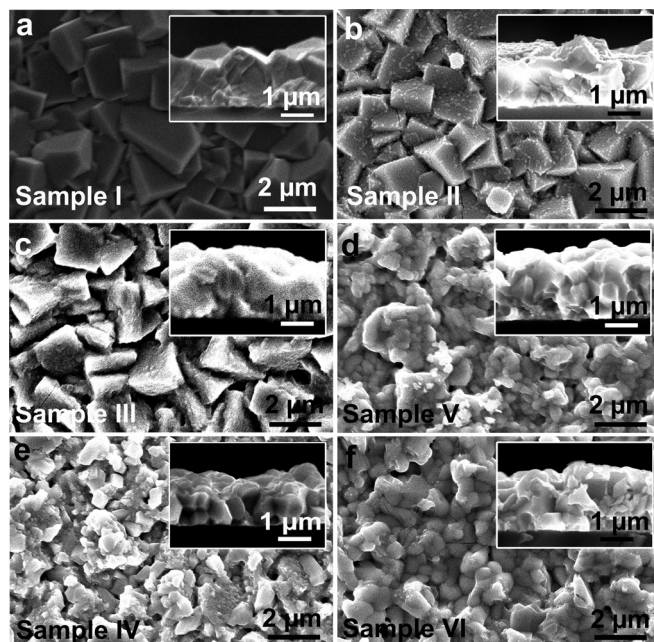


FIG. 1. Top-and side (inset)-view SEM images of as-grown (a) and sensitized PbSe annealed at 380 °C in (b) pure nitrogen for 30 min, (c) 20-min nitrogen followed by 10-min oxygen, (d) 25-min nitrogen followed by 5-min iodine, (e) pure oxygen for 30 min, and (f) 25-min oxygen followed by 5-min iodine.

including 30-min pure nitrogen (sample II), 20-min nitrogen followed by 10-min oxygen (sample III), 30-min pure oxygen (sample IV), 25-min nitrogen followed by 5-min iodine (sample V), 25-min oxygen followed by 5-min iodine (sample VI), mixed oxygen and iodine for 5 min (sample VII), and 15-min nitrogen followed 10-min oxygen and 5-min iodine (sample VIII), respectively. The flow was kept a constant of 0.05 psi. Both hot probe and Hall measurement show that the all as-grown and after-annealing samples are p-type. 200 nm thick gold thin films were then deposited by thermal evaporation over two sides of the PbSe detectors with a  $2 \times 2 \text{ mm}^2$  active area. The detectivity measurements were performed at room temperature (298 K) using a Model SR830 DSP lock-in amplifier and a collimated black-body at 500 K from Infrared System Development Corp., chopped at 750 Hz (MC1F10 from Thorlabs). The devices were biased at 100 V using Agilent E3612A source, with a load resistor matched to the sensor resistance.

## III. RESULTS AND DISCUSSION

Table I summarizes our experimental results on the sensitization of uncooled PbSe infrared photoconductive detectors. First, a high peak directivity up to  $1.0 \times 10^{10} \text{ cm} \cdot \text{Hz}^{1/2} \cdot \text{W}^{-1}$  was observed by annealing p-type PbSe microcrystalline films obtained from CBD in nitrogen and iodine atmosphere without oxygen. Second, the combined use of iodine and oxygen could further enhance the PbSe detectivity to two times larger ( $2.8 \times 10^{10} \text{ cm} \cdot \text{Hz}^{1/2} \cdot \text{W}^{-1}$ ) than those sensitized in iodine and nitrogen. This shows that oxygen can significantly improve the PbSe sensitivity. Third and most importantly, without iodine no photo-response was obtained from PbSe samples annealed in any atmospheres including in pure oxygen, indicating that it is iodine instead of oxygen that is really the key in activating the PbSe photo-response. In addition to the annealing atmosphere, sufficient annealing time at high temperature (above 360 °C) is also crucial for high photo-response.

To understand and clarify these results, we performed PL studies on the first seven samples listed in Table I. The room temperature PL emission spectra shown in Figure 2 were characterized by a Fourier transform infrared (FTIR) spectrometer in Step-Scan mode with a 1.064 μm Q-switched Nd:YAG pumping laser ( $\tau$  pulse = 5 ns, 10 Hz). No PL emission is observed in as-grown p-type PbSe film (Figure 2(a), sample I). After the annealing process, however, PL peaks emerge in all annealed PbSe films, as shown in Figures 2(b) to 2(g), though there are significant differences in their PL intensities. PL intensity of pure-nitrogen annealed PbSe film (Figure 2(b), sample II) is comparable with that with pure oxygen (Figure 2(d), sample IV). Oxygen annealing after nitrogen annealing significantly increases the PL intensity (Figure 2(c), sample III). On the contrary, PL intensity dramatically decreases after introducing iodine and iodine in oxygen causes a more rapid PL degradation than iodine in nitrogen, as shown in Figure 2(e) (sample V) and Fig. 2(f) (sample VI), respectively.

There are essentially four factors that dominate the PL intensities: material gain, loss mechanisms in Eq. (1)

TABLE I. Characterizations of uncooled PbSe detectors under various sensitization processes (active area:  $2 \times 2$  mm and bias voltage: 50 V/cm).

Samples#	Annealed atmosphere	Resistance (M $\Omega$ )	Responsibility at $\lambda_p$ (V/W)	D <sup>b</sup> ( $\lambda_p$ , 750, 1) (cm Hz <sup>1/2</sup> W <sup>-1</sup> )
Sample I	As-grown	0.02	a	a
Sample II	Nitrogen	0.05	a	a
Sample III	Nitrogen/oxygen	0.06	a	a
Sample IV	Oxygen	0.1	a	a
Sample V	Nitrogen/iodine	2.0	$1.8 \times 10^4$	$1.0 \times 10^{10}$
Sample VI	Oxygen/iodine	4.0	$3.1 \times 10^4$	$2.8 \times 10^{10}$
Sample VII	Oxygen + iodine <sup>b</sup>	2.0	$5.9 \times 10^3$	$1.2 \times 10^9$
Sample VIII	Nitrogen/oxygen/iodine	2.5	$2.9 \times 10^4$	$2.5 \times 10^{10}$

<sup>a</sup>No signal was obtained.

<sup>b</sup>Baked for 5 min.

including surface/interface recombination, extraction efficiency, and the effective pumping due to the diffuse pumping light.<sup>14</sup> As well known, compared with high-temperature physical methods such as MBE, a big drawback of CBD technique is lower crystal quality due to the numbers of intrinsic defects, such as lead vacancies ( $V''_{Pb}$ ) and selenium interstitials ( $Se_i^\cdot$ ) (as-grown PbSe is *p-type* in our case). These defects are attributed to the low growth temperature and the impurity containments from the aqueous precursors. It was reported that oxygen and sodium ion may be incorporated into PbSe films during the deposition process to form  $(X_x Pb_{1-x})(Y_y Se_{1-y})$ ,<sup>17,18</sup> where X stands for metal impurity and Y stands for non-metal impurity. However, a part of defects could vanish by a recrystallization process during high temperature annealing, which improves the crystal quality. Therefore, the occurrence of PL peaks after annealing is a good incitation of improved crystal quality. This is confirmed by the higher x-ray diffraction (XRD), peak intensity (Cu, K $\alpha$ , ROGAKU, D/MAX-2550V), and narrower full width at half maximum (FWHM) of PbSe (200) peak annealed in oxygen followed by iodine atmosphere, as shown in Figure 3.

The quality of recrystallization is determined by annealing temperature, time, and atmosphere. Since annealing

temperature and total annealing time are kept the same, the significant differences in PL peak intensities after annealing must be caused by the different annealing atmospheres. Although blunted edges and boundaries were observed from the all SEM images of annealed samples, as shown in Figures 1(b)–1(f), the surface roughness of PbSe basically remains the same. Therefore, the differences in extraction efficiency and effective pumping could be ignored. Owing to its highly reactive nature, oxygen could first react with the  $V''_{Pb}$  and  $Se_i^\cdot$  defects located in surface of PbSe microcrystals via diffusion in rich-oxygen atmosphere. However, long-time oxygen annealing could result in a serious deviation from stoichiometry of PbSe microcrystals due to overreaction with  $Pb^{2+}$ , and  $Se^{2-}$ . It will also form  $PbSe_{1-x}O_x$ , even insulating PbO layers on the surfaces and boundaries of PbSe microcrystals. This crystal-phase transformation is generally observed in rich-oxygen sensitized PbSe process, regardless of synthetic methods.<sup>17</sup> In our case,  $PbSeO_3$  was detected in XRD pattern of the sensitized PbSe, as shown in Figure 3(b). Compared with pure nitrogen sensitized PbSe films (sample II), a more distinct boundary coalescent between adjacent PbSe microcrystal showing in Figure 1(f) (sample IV) and the increase resistance from 0.05 to 0.1 M $\Omega$  clearly verify

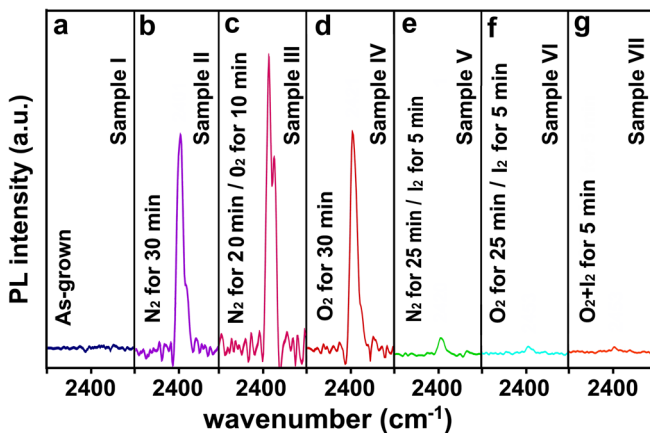


FIG. 2. PL spectra of as-grown (a) and sensitized PbSe films annealed at 380 °C in (b) pure nitrogen for 30 min, (c) 20-min nitrogen followed by 10-min oxygen, (d) pure oxygen for 30 min, (e) 25-min nitrogen followed by 5-min iodine, (f) 25-min oxygen followed by 5-min iodine, and (g) mixed oxygen and iodine for 5 min.

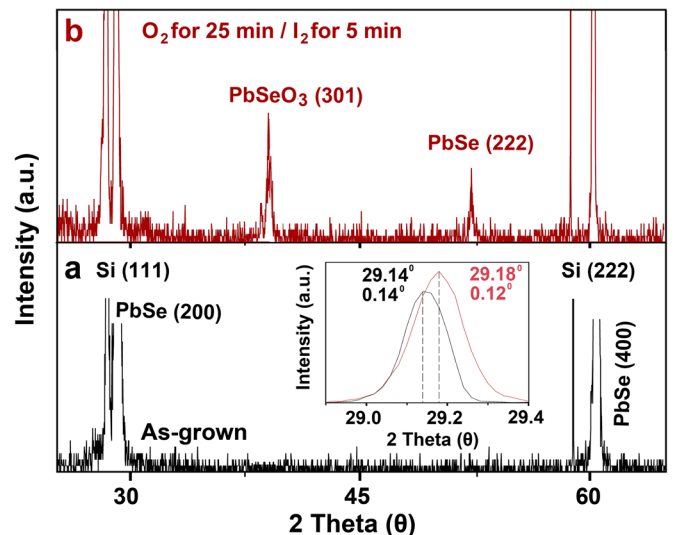


FIG. 3. XRD curves of (a) as-grown on Si substrate and (b) sensitized PbSe films annealed at 380 °C in 25-min oxygen followed by 5-min iodine atmosphere.

the oxidation process. Both stoichiometric deviation and over-oxidation lead to lattice defects, and thus degrade crystal quality. Therefore, we attribute the highest PL intensity on sample III with O<sub>2</sub> after N<sub>2</sub> annealing as a result of good combination of recrystallization and defect passivation.

However, no photo-response was observed in any sample of high PL intensity. Considering that photosensitivity is sensitive to microcrystal size, four 1.2 μm thick PbSe films with different microcrystal sizes ranging from 0.1 to 1.5 μm were fabricated. After annealing in pure oxygen atmosphere for 30 min, all samples show similarly much enhanced PL intensity as shown in Figure 4. However, no photo-response was observed on any of these four PbSe films, which confirms that oxygen alone does not sensitize *p*-type PbSe.

After introducing iodine to both the nitrogen (sample V) and oxygen (sample VI) annealed PbSe films for 5 min, high photo responses were observed and sample with oxygen annealing shows higher detectivity, as shown in Table I. Therefore, it is indisputable that iodine instead of oxygen plays a decisive role in photo-response of PbSe microcrystals. The comparison and analysis of PL and SEM images before and after introducing iodine could provide some useful guidelines for how the iodine triggers the sensitization of PbSe. First, a mechanism exists that iodine reduces the PL intensity significantly, as shown in Figure 2(e). Second, iodine further promotes the coalescence between PbSe crystals through fragmenting the large microcrystals into more numerous small ones with diameters in the range of 300–500 nm, resulting in blunted edges and boundaries of PbSe grains as shown in Figure 2(d). At the same time, the resistance increased by almost two orders of magnitude up to 2 MΩ. We believe that the changes mentioned above, which play the key role in the *p*-type PbSe sensitization, are attributed to the incorporation of iodine to PbSe, named iodination. However, no iodine element or iodine related phase was directly detected in our energy dispersive spectroscopy (EDS) and XRD measurements, indicating the concentration of iodine incorporated into PbSe is quite low.

A low detectivity of  $1.2 \times 10^9 \text{ cm} \cdot \text{Hz}^{1/2} \cdot \text{W}^{-1}$  was observed in PbSe sample annealed in oxygen followed by

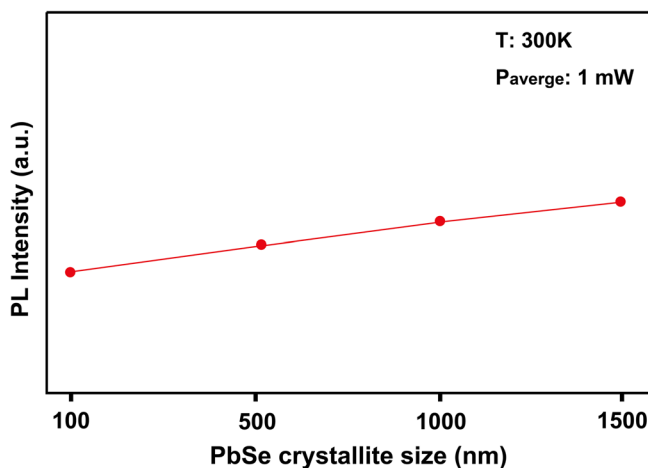


FIG. 4. PL spectra of sensitized PbSe with various sizes annealed at 380 °C in oxygen for 30 mins.

iodine totally for 5 min (sample VII). Compared with the high sensitivity of PbSe annealed in same atmosphere for 30 min (sample VI), the low sensitivity is attributed to the low crystal qualities before iodination due to insufficient recrystallization process, according to the PL results.

As an effective improver, the introduction of oxygen could dramatically enhance the sensitivity of PbSe. Based on the increased PL intensity in Figure 2(c), the enhanced sensitivity by introducing oxygen in nitrogen atmosphere before iodination (sample VIII) is attributed to the defect passivation by oxygen. The peak detectivity of  $2.8 \times 10^{10} \text{ cm} \cdot \text{Hz}^{1/2} \cdot \text{W}^{-1}$  was achieved by the combined use of oxygen and iodine (sample VI). It is a result of two reasons: (1) to form oxide layer in the boundary domain during oxidation; (2) to improve the incorporation of iodine into PbSe. The former is confirmed by the appearance of PbSeO<sub>3</sub> in XRD pattern (Figure 3(b)) of annealed PbSe sample in oxygen followed by iodine (sample V), and the latter is verified by the degraded PL intensity shown in Figure 2(f) and a more coalescent structure shown in Figure 1(f).

Based on the above results, we believe that the essence of *p*-type PbSe sensitization process for a high sensitivity is (1) to incorporate iodine into PbSe during the iodination process, (2) to increase crystal quality by high-temperature recrystallization process, and (3) to passivate defects and to introduce oxide layer in the boundary domain in rich oxygen atmosphere.

In light of the above equation, both iodine trap model and iodine induced *p*-*n* junction model could explain the significantly reduced PL intensity as discussed in the introduction. We would prefer the *p*-*n* junction model due to the following reasons. First, iodine is a *n*-type dopant in PbSe.<sup>19</sup> Recently, *n*-type iodine doped PbSe epitaxial layers were obtained on silicon substrates in our group by using MBE.<sup>20</sup> Second, based on the same reasoning from Eq. (1), our PL results do not support oxygen trap model since oxidation enhances instead hinders PL emission. Therefore, similar to that oxygen converts the *n*-type PbSe into *p*-type, *p*-*n* junction model could be applied for iodine sensitized *p*-type PbSe if *n*-type inversion region is formed at the outer layer of PbSe by introducing donor levels during iodination via diffusion process. Although Hall measurement on iodine annealed CBD PbSe still shows *p*-type conductivity, it could be that the *n*-type layer is very thin.

#### IV. CONCLUSION

In sum, we have studied the role of oxygen and iodine in *p*-type PbSe sensitization process. Although detailed sensitization mechanism still needs further study, it is clear that iodine instead of oxygen triggers the photo-responsibility of *p*-type PbSe. Oxygen serves as an efficient sensitization improver by defect passivation, forming oxide layers at the boundary domain and improving the iodination. Revisiting some of the old problems in IV–VI lead salt materials could lead to new and better understanding of these critical issues in Pb-salt materials, and could help introduce this process to other IV–VI devices such as light emitting devices and photovoltaic detectors.<sup>21,22</sup>

## ACKNOWLEDGMENTS

Funding for this work was partially provided by the DoD AFOSR under Grant No. FA9550-12-1-0451, DoD ARO Grant No. W911NF-07-1-0587, and by Oklahoma OCAST program under Grant Nos. AR112-18 and AR082-052.

- <sup>1</sup>A. Rogalski, *Infrared Detectors*, 2nd ed. (Taylor and Francis Group, LLC and CRC Press, 2011).
- <sup>2</sup>T. H. Johnson, *Proc. SPIE* **0443**, 60 (1983).
- <sup>3</sup>A. Muñoz, J. Meléndez, M. C. Torquemada, M. T. Rodrigo, J. Cebrián, A. J. de Castro, J. Meneses, M. Ugarte, F. López, G. Vergara, J. L. Hernández, J. M. Martín, L. Adell, and M. T. Montojo, *Thin Solid Films* **317**, 425 (1998).
- <sup>4</sup>Y. Yasuoka and M. Wada, *Jpn. J. Appl. Phys., Part 1* **13**, 1797 (1974).
- <sup>5</sup>F. Briones, D. Golmayo, and C. Ortíz, *Thin Solid Films* **78**, 385 (1981).
- <sup>6</sup>R. M. Candea, R. Turcu, G. Borodi, and I. Bratu, *Phys. Status Solidi A* **100**, 149 (1987).
- <sup>7</sup>R. L. Petritz, *Phys. Rev.* **104**, 1508 (1956).
- <sup>8</sup>*Narrow-Gap Semiconductors*, Springer Tracts in Modern Physics Series Vol. 98, edited by R. Dornhaus, G. Nimtz, B. Schlicht (Springer-Verlag, 1983), pp. 100–108.
- <sup>9</sup>H. Zogg, W. Vogt, and W. Baumgartner, *Solid-State Electron.* **25**, 1147–1155 (1982).
- <sup>10</sup>P. R. Emtage, *J. Appl. Phys.* **47**, 2565 (1976).
- <sup>11</sup>O. Ziep and M. Mocker, *Phys. Status Solidi B* **98**, 133 (1980).
- <sup>12</sup>S. Horn, D. Lohrmann, P. Norton, K. McCormack, and A. Hutchinson, *Proc. SPIE* **5783**, 401 (2005).
- <sup>13</sup>V. T. Trofimov, G. Yu, and E. G. Chizhevskii, *Fiz. Tekh. Poluprovodn. (S.-Peterburg)* **30**, 755 (1996).
- <sup>14</sup>F. Zhao, S. Mukherjee, J. Ma, D. Li, S. L. Elizondo, and Z. Shi, *Appl. Phys. Lett.* **92**, 211110 (2008).
- <sup>15</sup>J. N. Humphrey and R. L. Petritz, *Phys. Rev.* **105**, 1736 (1957).
- <sup>16</sup>J. N. Humphrey and W. W. Scanlon, *Phys. Rev.* **105**, 469 (1957).
- <sup>17</sup>M. C. Torquemada, M. T. Rodrigo, G. Vergara, F. J. Sánchez, R. Almazán, M. Verdú, P. Rodríguez, V. illamayor, L. J. Gómez, and M. T. Montojo, *J. Appl. Phys.* **93**, 1778 (2003).
- <sup>18</sup>M. A. Barote, B. D. Ingale, R. V. Suryawanshi, T. V. Chavan, and E. U. Masumdar, *Res. J. Chem. Sci.* **1**, 48 (2011).
- <sup>19</sup>S. Espevik, C. Wu, and R. H. Bube, *J. Appl. Phys.* **42**, 3513 (1971).
- <sup>20</sup>B. Weng, J. Qiu, Z. Yuan, and Z. Shi, “N-type iodine doped PbSe epitaxial layer fabricated by molecular beam epitaxy,” *J. Appl. Phys.* (unpublished).
- <sup>21</sup>B. Weng, J. Ma, L. Wei, L. Li, J. Qiu, J. Xu, and Z. Shi, *Appl. Phys. Lett.* **99**, 221110 (2011).
- <sup>22</sup>H. Zogg, K. Alchalabi, D. Zimin, K. Kellermann, and W. Buttler, *Nucl. Instrum. Methods Phys. Res. A* **512**, 440 (2003).